

DESIGN OF AN ULTRA-WIDEBAND, LOW-NOISE AMPLIFIER USING A SINGLE TRANSISTOR: A TYPICAL APPLICATION EXAMPLE

S. Demirel, F. Güneş, and U. Özkaya

Electronics and Communication Engineering Department
Yıldız Technical University
Beşiktaş, İstanbul, Turkey

Abstract—In this work, a design method of an Ultra-Wideband (UWB), low-noise amplifier (LNA) is proposed exerting the performance limitations of a single high-quality discrete transistor. For this purpose, the compatible (Noise F , Input VSWR V_i , Gain G_T) triplets and their (Z_S , Z_L) terminations of a microwave transistor are exploited for the feasible design target space with the minimum noise $F_{\min}(f)$, maximum gain $G_{T\max}(f)$ and a low input VSWR V_i over the available bandwidth B . This multi-objective design procedure is reduced into syntheses of the Darlington equivalences of the $Z_{S\text{opt}}(f)$, $Z_{L\max}(f)$ terminations with the Unit-elements and short-circuited stubs in the T -, L -, Π -configurations and Particle Swarm Intelligence is successfully implemented as a comparatively simple and efficient optimization tool into both verification of the design target space and the design process of the input and output matching circuits. A typical design example is given with its challenging performance in the simple Π - and Π -configurations realizable by the microstrip line technology. Furthermore the performances of the synthesized amplifiers are compared using an analysis programme in MATLAB code and a microwave system simulator and verified to agree with each other.

1. INTRODUCTION

Nowadays, microwave amplifier design is doubtlessly one of the major interests of microwave engineering. Considering all the stringent requirements which include high gain, low input VSWR together with the low-power consumption from the low-battery, the wideband miniature Low Noise Amplifier (LNA) design is one of the biggest

Corresponding author: F. Güneş (gunes@yildiz.edu.tr).

challenges to Ultra-Wideband (UWB) transceiver integrations. In order to meet these stringent requirements, first of all, the fast and low-noise, high quality transistors are needed, which is of course the matter of the available technology. Traditionally, wideband microwave amplifiers relied on transistors realized with composite semiconductors, e.g., GaAs, because of the intrinsic superior frequency characteristics of such devices [1–3]. The second level of the challenge is the rigorous analysis of performance capabilities for the chosen transistor in order to obtain the, then to design the microwave amplifier subject to this feasible design target space. Otherwise is to utilize the device either under its potential performance or for unrealizable requirements. This device characterization problem is solved point by point in [4, 5] on the rigorous mathematical bases throughout the operation domain within the physical limitations of the employed device. Then, combining this performance characterization with the Artificial Neural Networks (ANN) or Support Vector Regression Machine (SVRM) model of the device [6, 7], the compatible $[F, V_i, G_T]$ triplets together with their source Z_S and load Z_L terminations can be obtained as the functions of the operation variables V_{DS} , I_{DS} , f of the device (Fig. 1). Briefly, these compatible performance triplet functions outputted from the block diagram in Fig. 1 enable a designer all the necessary information to form a feasible design target space satisfying the requirements subject to the device potential performance characteristics. Here it should be noted that since all the solution terminations always take place within the Unconditionally Stable Working Area (USWA), stability of the device does not need to be considered as an additional target,

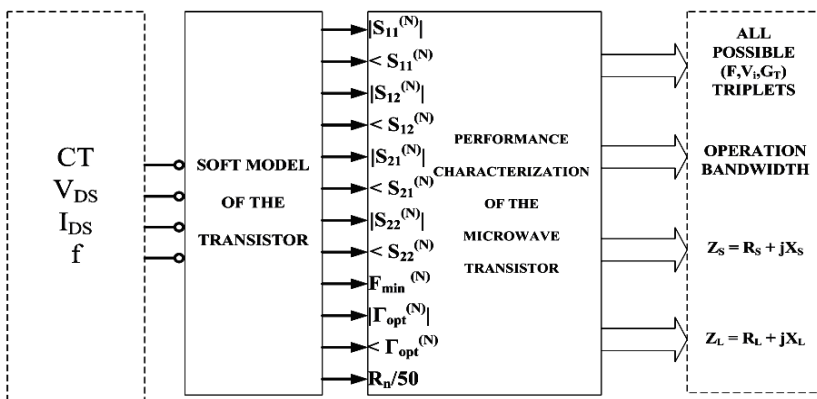


Figure 1. A block diagram for the compatible performance triplets of a microwave transistor.

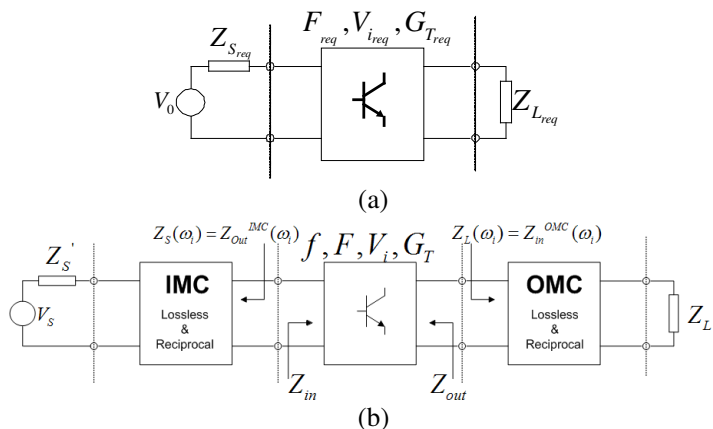


Figure 2. (a) Transistor with the compatible performance terminations. (b) Transistor with the Darlington equivalencies of the $Z_S(\omega), Z_L(\omega)$ terminations.

because it is taken into account within the concept of USWA at each operation frequency [4, 5]. Thus, from the respect of the feasible design target, the transistor can be represented by a two-port characterized by a chosen compatible $[F, V_i, G_T]$ triplet with its source and load terminations (Z_S, Z_L) as given by Figs. 2(a) and 2(b).

In this work, considering all the stringent requirements mentioned before, the performance limitations of a chosen high technology microwave transistor are employed in the determination of the design target space. Thus, the design procedure can briefly be summarized in the following stages:

(i) In the first stage, an UWB transistor with the ultra low noise characteristics is selected and its compatible $[F \min(f), V_i = \text{const.}, G_T \max(f)]$ triplets and the $[Z_{S_{opt}}(f), Z_{L_{max}}(f)]$ termination functions are obtained depending on device operation conditions, by applying the process given in the block diagram in Fig. 1. In this stage, firstly the bias condition V_{DS}, I_{DS} should be determined, then the minimum noise figure $F_{\min}(f)$, the maximum gain $G_{T_{\max}}(f)$ characteristics are investigated taking as the $V_i \geq 1$ a parameter (Figs. 5(a) and 2(b)) to decide the most suitable gain characteristic with the widest bandwidth and the low power consumption. In a recent work [8], considering the wireless transceiver front-end with antenna and propagation channel, it has been verified that the unflat-gain low-noise amplifier with an incremental gain characteristic does not degrade the performance of overall system. In the same work [8], as an alternative to its flat-gain

counterpart, the proposed unflat gain requirement has been shown to tolerate gain ripple as large as 10 dB, which greatly eases the design challenges to low-noise amplifier for UWB wireless receivers. Thus, the selection process for a $[F_{\min}(f), V_i = V_{i\text{req}} = \text{constant}, G_{T\text{max}}(f)]$ triplets can be achieved easily with its $Z_{S\text{opt}}(f), Z_{L\text{max}}(f)$ terminations over the possible widest bandwidth and low power as the feasible design process.

(ii) In the second stage, the multi-objective optimization process for the $[F_{\min}(f), V_i = V_{i\text{req}} = \text{constant}, G_{T\text{max}}(f)]$ triplets is reduced to only the scalar gain optimization of the two passive, reciprocal matching two-ports (Figs. 3(a) and 3(b));

(iii) Final stage is to choose the optimization algorithm. In fact, authors have experienced many algorithms with gradients/heuristics approaches [9–11] in the circuit synthesis process; in this work, “Particle Swarm Optimization” (PSO) algorithm is employed as a simple and efficient by the derivative-free optimization tool in the syntheses process of the matching networks. In fact, nowadays evolutionary optimization algorithms have applied a wide range of electromagnetic problems, such as genetic optimization of the wide-band multimodal square horns for discrete lenses [12] and diffusion coefficient of the turbulent jet [13] PSO design of the electromagnetic absorbers [14], PSO synthesis of the phased arrays [15], cylindrical conformal arrays [16] and smart antennas [17], null placement and side lobe reduction of the radiation patterns for the linear arrays using the ant colony optimization [18]. On the other hand some

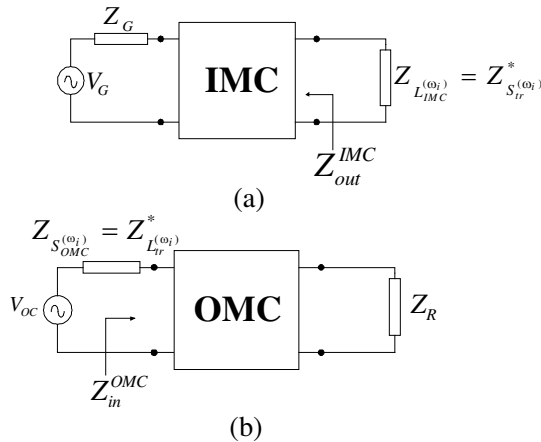


Figure 3. (a) Input matching circuits for the gain optimization. (b) Output matching circuits for the gain optimization.

culled hybrid approaches are generated to obtain more qualified algorithms for optimization problems: i.e., Initialization problem of the gradient-based algorithms are overcome by a good global optimum searcher PSO in [19]; in [20] combination of the GA with the PSO gives faster and more accurate results. Furthermore, in [21], PSO is employed with together the moment methods for design of the planar inverted-F antennas. Here, we apply a simple PSO to the constrained optimization within the synthesis problem of the distributed-parameter matching networks of the amplifier with a fast convergence. Moreover, by means of constraining the lower and upper bounds of the optimization variables in the feasible ranges of the planar transmission line technology, the synthesized amplifiers can result in the feasible circuits, which in our case can be realized by the microstrip technology.

Organization of the paper is as follows: In next section, design problem of a microwave amplifier is defined within the respects of this work; the third section is devoted to the optimization tool which is the particle swarm process. Typical amplifier design examples are given employing the microwave transistor ATF36077 in the fourth section, which is a 2–18 GHz Ultra Low Noise Pseudomorphic HEMT, finally the paper ends with the conclusions.

2. AMPLIFIER DESIGN PROBLEM

2.1. The Feasible Design Target Space: Compatible (F, V_i, G_T) Triplets and the (Z_S, Z_L) Terminations over an Available Operation Bandwidth B

In a typical design problem of a basic microwave amplifier employing per se a FET as an active device, the active device can be represented by a two-port. Since in such a system, all the main performance components of F, V_i, G_T are determined by the active device employed, so this necessitates that device be identified by all its compatible (F, V_i, G_T) performance triplets and their (Z_S, Z_L) terminations in its operation domain. The block diagram in Fig. 1 consisting of the signal-noise black-box model and performance characterization of the transistor gives the FDTS which consists of the compatible (F, V_i, G_T) triplets together with their source Z_S , and load Z_L terminations as the functions of the operation variables V_{DS}, I_{DS}, f of the device. Furthermore, for a compatible (F, V_i, G_T) triplet (Fig. 2(a)) at a chosen point within the operation domain of the device, the Darlington equivalences of the Z_S and Z_L terminations in the front- and back-end matching networks can also be modeled (Fig. 2(b)), respectively. Here, the (Z_S, Z_L) terminations are the simultaneous solutions of the

following nonlinear performance equations of the transistor subject to the physical realization conditions [4, 5]:

$$F \triangleq \frac{(S/N)_i}{(S/N)_O} = F\{R_S, X_S\} = F_{\min} + \frac{R_N}{|Z_{\text{opt}}|^2} \frac{|Z_S - Z_{\text{opt}}|^2}{R_S}, \quad (1)$$

$$V_i \triangleq V_i\{R_S, X_S, R_L, X_L\} = \frac{1 + |\rho_i|^2}{1 - |\rho_i|^2}, \quad \rho_i = \frac{Z_S - Z_{\text{in}}^*}{Z_S + Z_{\text{in}}}, \quad (2)$$

$$G_T \triangleq \frac{P_L}{P_{AVS}} = G\{R_S, X_S, R_L, X_L\} = \frac{4R_S R_L |z_{21}|^2}{|(z_{11} + Z_S)(z_{22} + Z_L) - z_{12} z_{21}|^2} \quad (3)$$

Here the physical realization conditions can be expressed as follows: for $\text{Re}\{Z_S\} > 0$, $\text{Re}\{Z_L\} > 0$,

$$\text{Re}\{Z_{\text{in}}\} = \text{Re}\left\{z_{11} - \frac{z_{12} z_{21}}{z_{22} + Z_L}\right\} > 0, \quad (4)$$

$$\text{Re}\{Z_{\text{out}}\} = \text{Re}\left\{z_{22} - \frac{z_{12} z_{21}}{z_{11} + Z_S}\right\} > 0, \quad (5)$$

$$F \geq F_{\min}, \quad V_i \geq 1, \quad G_{T \min} < G_T \leq G_{T \max} \quad (6)$$

where $z_{ij} = r_{ij} + jx_{ij}$, $i, j = 1, 2$ are the open-circuited parameters of the transistor, and the conditions given by (4) and (5) ensures the stable operation of the active device.

2.2. Darlington Synthesis of the (Z_S, Z_L) Terminations

In synthesis of the (Z_S, Z_L) terminations, gains of the lossless and reciprocal matching circuits terminated by $Z_S^*(\omega)$ and $Z_L^*(\omega)$ as given in Figs. 3(a) and 3(b), respectively, are maximized with respect to the circuit parameters, respectively.

As worked examples, two-ports of the three commonly used, simple distributed-parameter topologies, which are T -, Π -, L - are chosen to match a given generator/load impedances which are 50Ω for our case, to the target Z_S & Z_L impedance variations in the target operation bandwidth. In these worked examples, FDVS is utilized by considering RF microelectronic technology. For this purpose optimization variables which are the physical lengths and characteristic impedances of the transmission lines, are constrained within their feasibility ranges of the commonly used transmission lines technology, e.g., in our case microstrip, in the employed particle swarm based algorithm.

Thus, the multi-objective design of the whole amplifier is simplified in two respects: (i) The whole optimization process is

reduced to only gain optimization of the two reciprocal, lossless, simple matching two-ports, each of which is to provide the target Z_S & Z_L termination of the required triplet to the transistor. (ii) Furthermore, gain optimization is achieved simple and very fast by particle swarm optimization which is briefly given in the next section.

3. OPTIMIZATION

3.1. Feasible Design Variables and Target Space

The following two subspaces have to be considered as the feasible design space for a microwave amplifier: (1) The FDVS for which two factors should be taken into account: (i) The operation bandwidth B that is considered in the FDTS too; (ii) The lower-and upper limitations of the technology employed to realize the circuit. For our case, the FDVSs (ϑ_{imc}), (ϑ_{omc}) can be defined for the IMC and OMC circuits, respectively:

$$(\vartheta_{imc}) = [\ell_i Z_{oi}]^t, \quad (\vartheta_{omc}) = [\ell_i Z_{oi}]^t \quad (7)$$

where ℓ_i physical length and Z_{oi} characteristic impedance sub-vectors are constrained within the feasible limitations of the RF/microwave planar transmission line technology, particularly microstripline technology, which form the corresponding solution space. (2) The FDTS is the following compatible triplet with its (Z_S , Z_L) terminations:

$$\begin{aligned} (F_{\text{req}} = F_{\text{min}}(f), \quad V_i = V_{i\text{req}} = \text{Const.}, \quad G_{T\text{max}}(f)) &\Leftrightarrow \\ Z_{S\text{opt}}(f) = R_{S\text{opt}}(f) + jX_{S\text{opt}}(f) & \\ Z_{L\text{max}}(f) = R_{L\text{max}}(f) + jX_{L\text{max}}(f) & \end{aligned} \quad (8)$$

Here, this performance triplet and its terminations are guaranteed to satisfy the performance equations given by (1)–(3) together with the physical realization conditions in (4)–(6) which takes into account the limitations of the device and stability of the circuit.

3.2. Particle Swarm Optimization and Application to the Amplifier Design Problem

The PSO algorithm is an evolutionary algorithm capable of solving difficult multidimensional optimization problems in various fields. Since its introduction in 1995 by Kennedy and Eberhart [8], the PSO has gained an increasing popularity as an efficient alternative to Genetic Algorithm (GA) and Simulated Annealing (SA) in solving optimization design problems in antenna arrays. As an evolutionary algorithm, the PSO algorithm is similar to GA, since it works with

population of individuals randomly initialized and calculates fitness computation after each step, updates of the population based on the fitness value and iterative algorithm stops when certain criteria are met [22]. However there are no cross-over nor mutation operations, in PSO to update the population, only the best particles are used. For an N -dimensional problem, the position X and velocity V can be specified by $M \times N$ matrices, where M is the number of particles in the swarm and each particle represents a possible solution to the optimization problem. The main steps of the PSO algorithm are shown in Fig. 4 in a flowchart diagram. After defining the design variable space and the fitness function, the PSO algorithm starts by randomly initializing the position and velocity of each particle in the swarm. The position matrix is updated at each iteration according to

$$X^t = X^{t-1} + V^t \quad (9)$$

where the superscripts t and $t - 1$ refer to the time index of the current and the previous iterations. To update the velocity matrix at each iteration, every particle should know its personal best and the global best position vectors. The personal best position of the i th particle is represented as $Pbest_i = (pbest_{i1}, pbest_{i2}, \dots, pbest_{iN})$. The global best position vector defines the position in the design variable space at which the best fitness value was achieved by all particles, and is defined by $Gbest = (gbest_1, gbest_2, \dots, gbest_N)$. Thus, all the information needed by the PSO algorithm is contained in X , V , $Pbest$ and $Gbest$. Then, the velocity in the n th dimension of the m th particle in (9) is updated according to [12],

$$v_{mn}^t = wv_{mn}^{t-1} + c_1U_{n1}^t (p_{bestmn}^t - x_{mn}^{t-1}) + c_2U_{n2}^t (g_n^t - x_{mn}^{t-1}) \quad (10)$$

where the superscripts t and $t - 1$ refer to the time index of the current and the previous iterations, U_{n1} and U_{n2} are two uniformly distributed random numbers in the interval $[0, 1]$ and these random numbers are different for each of the n components of the particle's velocity vector. The parameters c_1 and c_2 are learning factors that usually $c_1 = c_2 = 2$. The parameter w is a number, called the "inertial weight," in the range $[0, 1]$, and its large values favor to global search, whereas the small values favor for local search. Inertial weight w is typically initialized to a value close to 1 and decreased linearly during the execution of the algorithm.

As seen from (10), the core of the PSO algorithm is the method by which X , V , $Pbest$ and $Gbest$ are updated in every iteration of the optimization process. Therefore according to the flow chart in Fig. 4, at each iteration, fitness function value is computed for each particle and the each particle's personal best and global best value of the swarm are defined among these values. This convergence finishes

when the target value is met or the algorithm reaches its maximum iteration number.

We have two optimization problems in this work: The first is to verify $G_{T_{\max}}(f)$ and $Z_{L_{\max}}(f)$ resulted from the performance characterization of the device given by (8). For this purpose, the design variables consist of the real (R_L) and imaginary (X_L) parts of the load at each operation f frequency and the corresponding solution

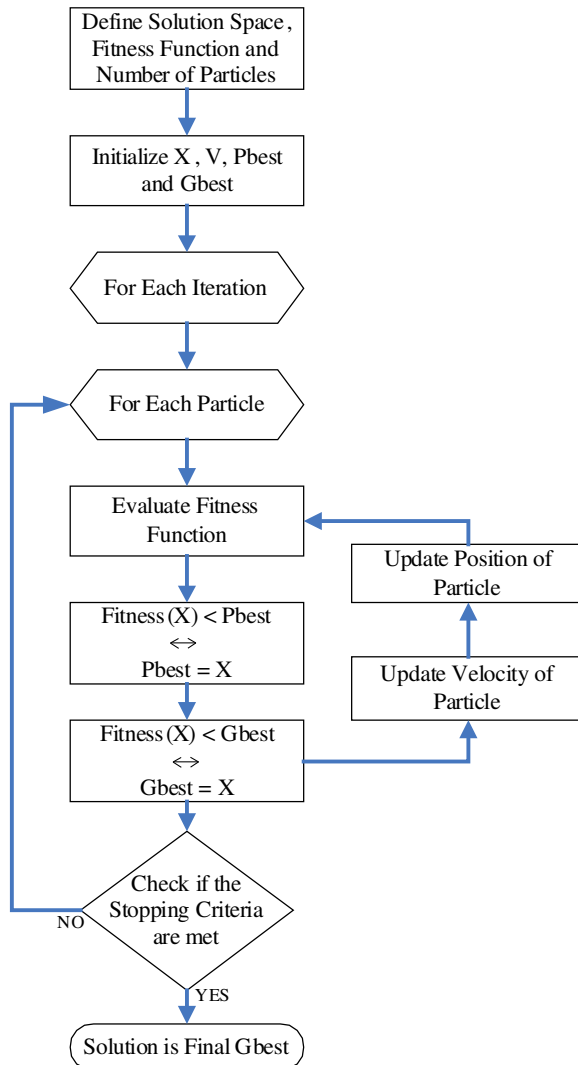


Figure 4. Flowchart of the PSO Algorithm.

space can be defined as $R_L > 0$ ensuring $\text{Re}\{Z_{\text{in}}\} > 0$ given by (4), since $Z_S = Z_{S_{\text{opt}}}$ is given as a noise parameter of the transistor at each operation frequency of the chosen bias condition in the modeling stage. Since this problem can be defined as a constrained maximization of the transistor gain G_T by $F_{\text{req}} = F_{\text{min}}$, $V_i = V_{i\text{req}} \geq 1$, therefore fitness for the algorithm may be defined as an error at each operation frequency as follows:

$$\varepsilon = e^{-aG_T} + b|V_i - V_{i\text{req}}| \quad (11)$$

where G_T and V_i are given by (3) and (2), respectively and Z_S is taken as equal to $Z_{S_{\text{opt}i}}$ to provide F_{min} at i th operation frequency. In (11), a and b are weighting coefficients and are taken as unity. For this problem, since the number of dimensions \Leftrightarrow the number of the design variables is 2, 20 particles are found to be sufficient for the fast convergence of the optimization process.

The second optimization problem is the Darlington design of the $Z_{S_{\text{opt}}}(f)$ and $Z_{L_{\text{max}}}(f)$ terminations. In this problem, we are interested in maximizing gain of a lossless and reciprocal, distributed parameter matching two-ports given in Figs. 3(a) and 3(b); hence since the maximum gain is equal to unity for the matching circuits, the following error function is used to evaluate the fitness:

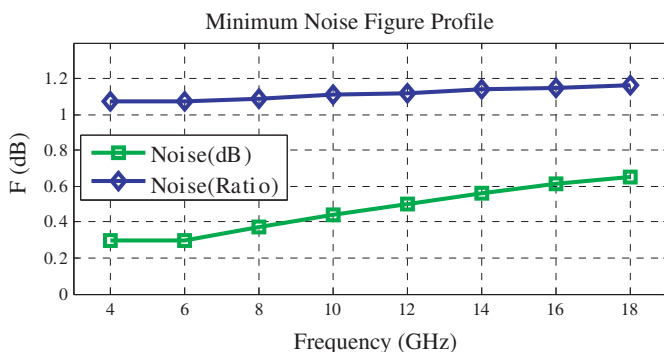
$$\varepsilon = \sum_i (1 - G_{T_i}(f_i, \vartheta)) \quad (12)$$

where G_{T_i} and ϑ are the transducer gain and distributed parameters of IMC or OMC, given by (3), (7) respectively. Since number of the design variables is increased in this problem, the number of the possible solution \Leftrightarrow the number of the particles is also increased, thus, 50 particles were used for the sufficiently fast convergence. Learning factors (c_1 , c_2) were set to 2, inertial weight was set to 0.9 and decreased linearly during the execution of the algorithm for both problems as mentioned before. Optimization process is completed as soon as iteration number reached to the maximum iteration number which is equal to 200 or the error value gets lower than 10⁻³. In our PSO design applications, optimization is completed as the iteration number changes between 80 and 20 depending on the initialization which takes as a computation time of 6.5 sec and 1 sec, respectively with Pentium 4 CPU, 3 GHz Processor, 512 MB RAM.

4. TYPICAL DESIGN EXAMPLES

In this work, ATF 36077 is chosen as a high-quality transistor to design microwave amplifiers and its scattering and noise parameters given by the manufacturer's data sheet [23] are utilized in the

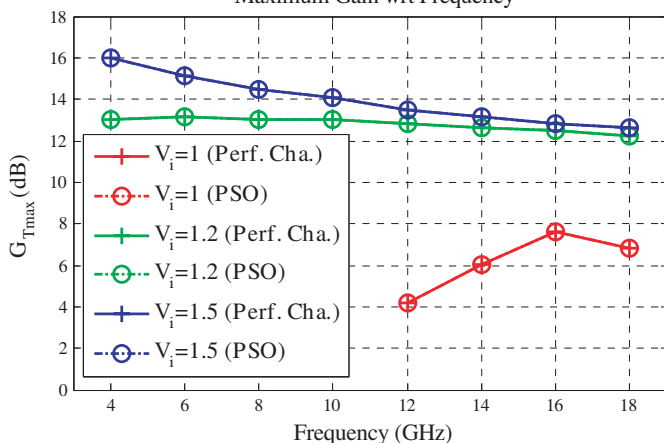
design process. Fig. 5(a) shows its guaranteed minimum noise figure $F_{\min}(f)$ by the manufacturer's data sheets and Fig. 5(b) gives the maximum gain profiles constrained by its minimum noise figure $F_{\min}(f)$ and the constant input VSWRs at each operation frequency, obtained from both the device performance characterization and the PSO using the objective function given by (11), respectively. Furthermore, Fig. 5(c) gives the source and load terminations ensuring the constrained maximum gain throughout the potential operation bandwidth. Investigating the gain — bandwidth characteristics in the Fig. 5(b), the $V_i = 1.2$ is chosen as an optimal value for the input mismatching and the Table 1 gives the load terminations together with their corresponding maximum gain values as the function of frequency, respectively, obtained by the performance characterization



(a)

$$(F_{\text{req}}=F_{\min}, V_i, G_{\text{Treq}}=G_{\text{Tmax}})$$

Maximum Gain wrt Frequency



(b)

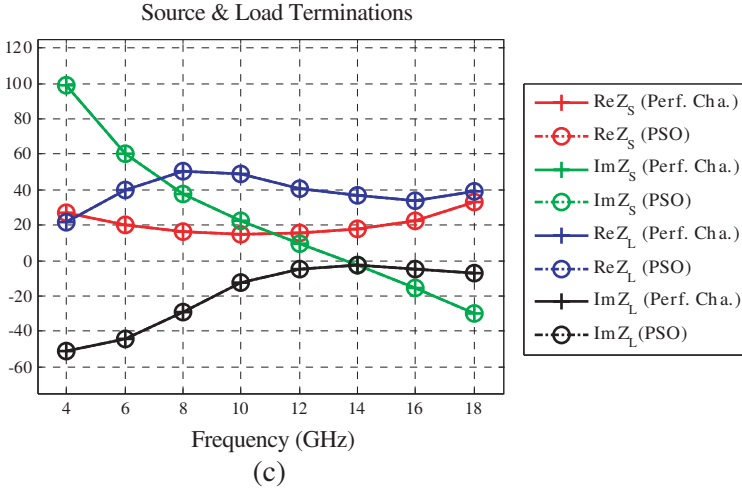


Figure 5. (a) Minimum noise profile for ATF 36077 at $V_{DS} = 2$ V, $I_{DS} = 10$ mA. (b) Maximum gain characteristics constrained by the minimum noise and input VSWR for ATF 36077. (c) Source and load terminations of the constrained maximum gain by $\{F_{\min}(f), V_{i\text{req}} = 1.2\}$.

and the PSO. The Unit element (ℓ, Z_0) and short-circuited stub (ℓ, Z_0) are utilized as distributed-parameter elements in T -, Π - and L -configurations in the matching circuits with the fitness given by (12). Here, the gain, noise and input VSWR performances of the most successful design are given in Figs. 6(a)–(c) respectively, compared with their targets and simulations. The solution space of the performances in Figs. 6(a)–(c) is given Table 2, which is constrained to be realizable by the microstrip technology. Furthermore the source and load impedance variations resulted from the solution space in the Table 2 are also compared in the Smith chart with the target and simulated variations in Fig. 7. As seen from the performance graphics in Figs. 6(a)–(c) and the impedance variations in Fig. 7, the synthesized values are verified by the professional microwave simulation programme. However, since the required terminations are not exactly provided, this results in achieving the smaller gain than the target at each operation frequency together with some amount of extra mismatching at the input port. In spite of this, a good noise performance is obtained as compared to the target all throughout the operation bandwidth as seen from the Fig. 6(c). All this synthesis process is achieved by a very efficient utilization of the PSO algorithm such as about within 30–40 iterations as seen from its typical convergence performance PSO in Fig. 8.

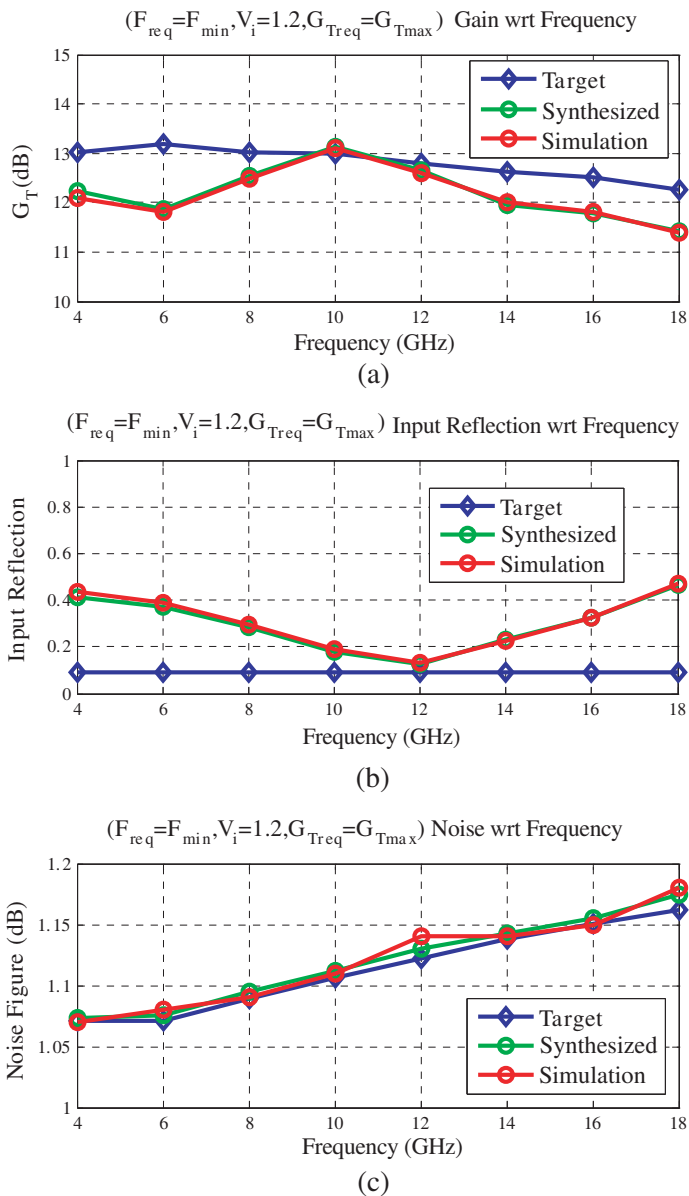


Figure 6. The resulted performance components compared with the target and simulated ones (Π - and Π -type).

Table 1. Maximum gain and load terminations for the triplets of $\{F_{\min}(f), V_{i\text{req}} = 1.2, G_{T\text{max}}(f)\}$.

f(GHz)	Performance Characterization			PSO		
	Re($Z_{L\text{max}}$) Ω	Im($Z_{L\text{max}}$) Ω	$G_{T\text{max}}$ (dB)	Re($Z_{L\text{max}}$) Ω	Im($Z_{L\text{max}}$) Ω	$G_{T\text{max}}$ (dB)
2	7,118	-48,036	12,438	7,139	-48,158	12,438
4	21,895	-50,933	13,023	21,337	-49,999	13,02
6	40,132	-44,142	13,178	40,536	-44,365	13,178
8	50,685	-29,04	13,024	50,234	-29,07	13,024
10	48,705	-12,252	12,992	48,986	-12,052	12,992
12	40,493	-4,762	12,792	40,752	-4,356	12,792
14	37,009	-2,819	12,623	36,951	-3,167	12,623
16	33,542	-4,795	12,513	33,444	-4,225	12,512
18	38,869	-7,034	12,256	38,963	-7,193	12,256

Table 2. Solution space for the IMC & OMC elements (II-II).

Type	ℓ_1 (cm)	ℓ_2 (cm)	ℓ_3 (cm)	Z_1 (Ω)	Z_2 (Ω)	Z_3 (Ω)
IMC	0.43	5.98	0.52	27.14	34.5	78.24
OMC	6.96	0.97	0.58	105.49	53.96	77.1

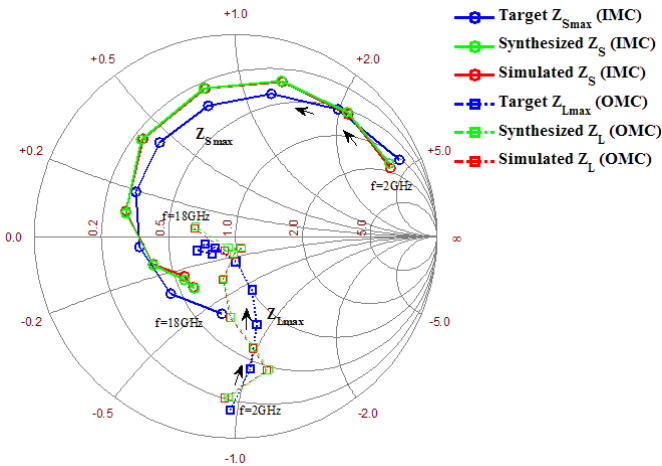


Figure 7. The source and load terminations for the (II- and II-) microwave amplifier for the triplet of $(F_{\text{req}} = F_{\min}(f), V_{i\text{req}} = 1.2, G_{T\text{req}} = G_{T\text{max}}(f))$.

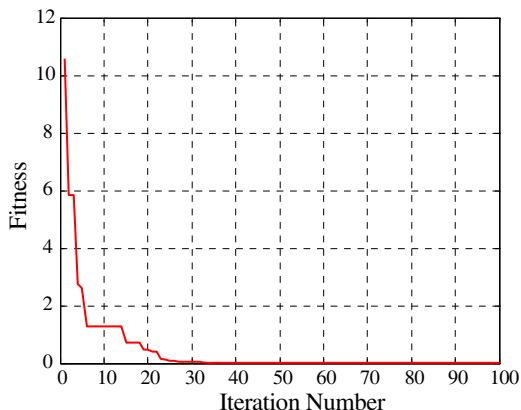


Figure 8. Typical convergence curve for the PSO design process.

5. CONCLUSION

In this work, a design process for the UWB amplifier is given using the performance limitations of the employed transistor which are the achievable minimum noise $F_{\min}(f)$, accompanying the maximum stable gain $G_{T\max}(f)$ over its largest available operation bandwidth B of the device at the expense of a small mismatching at the input port. This design target space is proved to be feasible using the compatible performance $[F, V_i, G_T]$ triplets together with their source Z_S and load Z_L terminations of the active device. The resulted multi-objective design procedure is reduced into syntheses of the Darlington equivalences of the target source $Z_{S\text{opt}}(f)$, load $Z_{L\max}(f)$ terminations using the Unit element and short-circuited stubs in L -, T -, Π -configurations. Besides, the Particle Swarm Intelligence is successfully implemented as a comparatively simple and efficient optimization tool. Typical design examples are presented here using ATF36077 with the matching circuits configured of the Π & Π forms. Furthermore, the solution spaces with their resulted performances together are given too. It can be concluded the suggested single transistor design is capable of the challenging performance compared with the counterparts employing two or more transistors in the complicated configurations.

REFERENCES

1. Mimino, Y., M. Hirata, K. Nakamura, K. Sakamoto, Y. Aoki, and S. Kuroda, "High gain-density K-band P-HEMT LNA MMIC

- for LMDS and satellite communication,” *IEEE Radio Frequency Integrated Circuits Symp.*, 209–212, 2000.
2. Trotta, S., H. Knapp, K. Aufinger, T. F. Meister, J. Böck, B. Dehlink, W. Simbürger, and A. L. Scholtz, “An 84 GHz bandwidth and 20 dB gain broadband amplifier in SiGe bipolar technology,” *IEEE J. Solid-state Circuits*, Vol. 42, No. 10, 2099–2106, Oct. 2007.
 3. Li, Q. and Y. P. Zhang, “A 1.5 V 2–9.6 GHz inductorless low-noise amplifier in 0.13 μm CMOS,” *IEEE Trans. on Microwave Theory and Techniques*, Vol. 55, No. 10, 2015–2024, Oct. 2007.
 4. Güneş, F., M. Güneş, and M. Fidan, “Performance characterisation of a microwave transistor,” *IEE Proceedings — Circuits, Devices and Systems*, Vol. 141, No. 5, 337–344, Oct. 1994.
 5. Güneş, F. and B. A. Çetiner, “A novel smith chart formulation of performance characterisation for a microwave transistor,” *IEE Proceedings — Circuits Devices and Systems*, Vol. 145, No. 6, 419–428, 1998.
 6. Güneş, F., H. Torpi, and F. Gürgen, “A multidimensional signal-noise neural network model for microwave transistors,” *IEE Proceedings — Circuits Devices and Systems*, Vol. 145, No. 2, 111–117, Apr. 1998.
 7. Güneş, F., N. Türker, and F. Gürgen, “Signal-noise support vector model of a microwave transistor,” *Int. J. RF and Microwave CAE*, Vol. 17, No. 4, 404–415, Jul. 2007.
 8. Li, Q. and Y. P. Zhang, “Alternative approach to low-noise amplifier design for ultra-wideband applications,” *Int. J. RF and Microwave CAE*, Vol. 17, No. 2, 153–159, Mar. 2007.
 9. Güneş, F. and Y. Cengiz, “Optimization of a microwave amplifier using neural performance data sheets with genetic algorithms,” *Lecture Notes in Computer Science*, 630–637, 2003.
 10. Cengiz, Y., H. Göksu, and F. Güneş, “Design of a broadband microwave amplifier using neural performance data sheets and very fast simulated reannealing,” *Lecture Notes in Computer Science*, Vol. 6, No. 2, 815–820, 2006.
 11. Güneş, F. and S. Demirel, “Gain gradients applied to optimization of distributed-parameter matching circuits for a microwave transistor subject to its potential performance,” *Int. J. RF and Microwave CAE*, Vol. 18, 99–111, 2008.
 12. Agastra, E., G. Bellaveglia, L. Lucci, R. Nesti, G. Pelosi, G. Ruggerini, and S. Selleri, “Genetic algorithm optimization of high-efficiency wide-band multimodal square horns for discrete

- lenses,” *Progress In Electromagnetics Research*, PIER 83, 335–352, 2008.
13. Ngo Nyobe, E. and E. Pemha, “Shape optimization using genetic algorithms and laser beam propagation for the determination of the diffusion coefficient in a hot turbulent jet of air,” *Progress In Electromagnetics Research B*, Vol. 4, 211–221, 2008.
 14. Chamaani, S., S. A. Mirta, M. Teshnehlab, M. A. Shooredeli, and V. Seydi, “Modified multi-objective particle swarm optimization for electromagnetic absorber design,” *Progress In Electromagnetics Research*, PIER 79, 353–366, 2008.
 15. Li, W.-T., X.-W. Shi, and Y.-Q. Hei, “An improved particle swarm optimization algorithm for pattern synthesis of phased arrays,” *Progress In Electromagnetics Research*, PIER 82, 319–332, 2008.
 16. Lu, Z.-B., A. Zhang, and X.-Y. Hou, “Pattern synthesis of cylindrical conformal array by the modified particle swarm optimization algorithm,” *Progress In Electromagnetics Research*, PIER 79, 415–426, 2008.
 17. Mahmoud, K. R., M. El-Adawy, S. M. M. Ibrahim, R. Bansal, and S. H. Zainud-Deen, “A comparison between circular and hexagonal array geometries for smart antenna systems using particle swarm optimization algorithm,” *Progress In Electromagnetics Research*, PIER 72, 75–90, 2007.
 18. Hosseini, S. A. and Z. Atlasbaf, “Optimization of side lobe level and fixing quasi-nulls in both of the sum and difference patterns by using continuous ant colony optimization (ACO) method,” *Progress In Electromagnetics Research*, PIER 79, 321–337, 2008.
 19. Ghaffari-Miab, M., A. Farmahini-Farahani, R. Faraji-Dana, and C. Lucas, “An efficient hybrid swarm intelligence-gradient optimization method for complex time Green’s functions of multilayer media,” *Progress In Electromagnetics Research*, PIER 77, 181–192, 2007.
 20. Li, W.-T., X.-W. Shi, L. Xu, and Y.-Q. Hei, “Improved GA and PSO culled hybrid algorithm for antenna array pattern synthesis,” *Progress In Electromagnetics Research*, PIER 80, 461–476, 2008.
 21. Su, D., D.-M. Fu, and D. Yu, “Genetic algorithms and method of moments for the design of PIFAS,” *Progress In Electromagnetics Research Letters*, Vol. 1, 9–18, 2008.
 22. Kennedy, J. and R. C. Eberhart, “Particle swarm optimization,” *Proc. IEEE Conf. Neural Networks IV*, Piscataway, NJ, 1995.
 23. www.agilent.com.